JOURNAL OF MATERIALS SCIENCE 33 (1998) 2771–2779

Effects of heat treatments on the ductility of cobalt electrodeposits

J. DILLE, J. CHARLIER, R. WINAND*
*Métallurgie Physique, CP 194/3, and *Métallurgie Electrochimie, CP 165, Université Libre de Bruxelles, Avenue F.D. Roosevelt, 50–B1050 Bruxelles, Belgium*
E-mail: jdille@ulb.ac.be

The effects of annealing treatments on the structure and mechanical properties of cobalt electrodeposits have been studied. Annealing temperatures range from 250–800 °C, i.e. below, as well as above, the allotropic α-h c p ⇌ β-f c c transformation temperature (417 °C). The structural characterization included hydrogen content measurement, relative volume fraction of α and β phases determination by X-ray diffraction, and microstructural investigations by optical and electron microscopy. The results showed that an annealing is a very effective means to optimize the ductility of cobalt electrodeposits. The increase of ductility observed after annealing is essentially due to a decrease of the stacking fault density in the deposits. Annealing treatment above the allotropic transformation temperature also produces, in some deposits, an increase of the ductile β-f c c phase content, but this fact does not lead to supplementary improvements of ductility. This is due to the detrimental influence of hydrogen that always exists in these deposits.

1. Introduction

The limited number of slip systems in α-h c p cobalt phase restricts its ductility. This lack of ductility makes the production of cobalt foils by thermomechanical process difficult [1–3]. Furthermore, the ductility of the final product is often below the requirements for most applications. By alloying cobalt with different elements, such as iron and nickel, the β-f c c structure with more slip systems can be stabilized and then the ductility of cobalt is increased.

Cobalt thin strips are fabricated from metal powder using powder rolling techniques primarily for the manufacture of cored welding wire for hard surfacing. These cobalt strips are alloyed with iron and nickel. On the other hand, these elements usually have a detrimental effect on the properties of hard-faced deposits when their amount reaches an initial level [1].

Electrodeposition of cobalt foils allows the thermomechanical processes to be avoided and the foil to be obtained directly at its final thickness. Unfortunately, electrodeposited materials generally suffer a lack of ductility compared with cast and wrought products. This fact makes the use of electrolytic cobalt foils difficult. However, suitable annealing treatments seem to be a promising route to improve the ductility of cobalt electrodeposits [4].

The purpose of the present work was to investigate the effects of heat treatments on the structure and the mechanical properties of free-standing cobalt electrodeposits with a particular emphasis on the ductility [5]. The study was limited to pure cobalt foils. The effect of iron or nickel codeposition will be described in a further publication.

In order to reach the objectives of this work, different cobalt electrodeposits displaying the most frequently encountered structures were required. This was achieved by varying the electrolyte pH value over a wide range. The deposits should be thick enough for their mechanical properties to be unaffected by the substrate-influenced deposit zone. Pure cobalt undergoes a martensitic α-h c p ⇌ β-f c c phase transformation. The α-h c p phase is thermodynamically stable up to 417 °C, whereas the β-f c c phase is stable at temperatures higher than 417 °C. In this study the annealing temperature range extended from 250–800 °C, i.e. below, as well as above, the allotropic transformation temperature.

2. Experimental procedure

2.1. Material

Cobalt foils were electrodeposited in a channel cell in order to control the hydrodynamics during the deposition. An additive-free electrolyte containing 202 g dm^{-3} $CoCl_2 \cdot 6H_2O$ (0.85 Co^{2+}) was flowed parallel to the electrodes with a flow rate of 0.4 m s^{-1}.

The commercially pure copper cathode was polished using 600 grade abrasive paper and then carefully cleaned with ethanol. The anode was a pure cobalt electrode.

The cobalt electrodeposits were obtained at a constant current density of 800 A m^{-2}. The temperature of the electrolyte was kept at 50 °C, and the electrolyte

0022–2461

pH values ranged from 1.0–5.0 and were adjusted by HCl additions.

The deposits were about 200 μm thick, and were separated from the substrate in order to obtain free-standing foils.

Depending on the electrolyte pH value, two types of cobalt electrodeposits were obtained. Their structures, detailed in a previous paper [4], were completely different in that:

1. the first type of deposit obtained at pH > 3.0 was a field-oriented texture (FT) type. Its columnar structure consisted of narrow prismatic crystallites with a strong α-h c p (1 1 $\bar{2}$ 0) preferred orientation; the surface of these satin-like or pale-grey deposits was relatively smooth; Fig. 1a shows a transmission electron micrograph of a thin foil parallel to the substrate;

2. the second type of deposit, obtained at pH < 3.0 consisted of an assembly of dihedran with nearly random crystallographic orientation; the surface of these dull dark-grey or black deposits was rather rough. Fig. 1b shows a transmission electron micrograph of a thin foil parallel to the substrate.

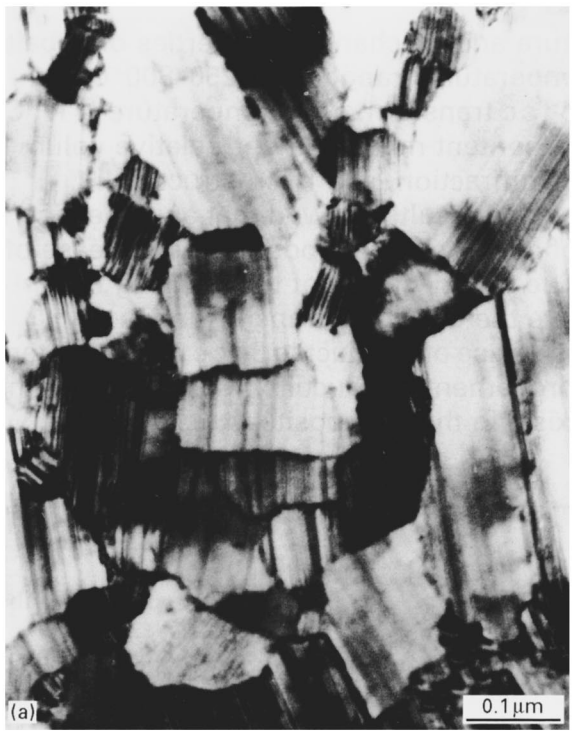

Figure 1 Transmission electron micrograph of as-electrodeposited cobalt specimens. Sections parallel to the substrate: (a) deposit obtained at pH 4, (b) deposit obtained at pH 1.5.

The ductility of the cobalt foils was tested by means of a tensile test and characterized by the elongation at fracture, A. The ductility of each kind of deposit was significantly different. The FT type of deposit had no ductility ($A < 1\%$) compared to the nearly randomly oriented cobalt electrodeposits for which the elongation, A, varied from 2%–6% when the pH of the electrolyte increased from 1.0–3.0. Nevertheless, the ductility of this second type of deposit remained rather low. Both types of electrodeposit were used in the present work. Their structural features, ductility and the electrolysis conditions are listed in Table I.

2.2. Heat treatments

Fig. 2 summarizes the various annealing temperatures (250–800 °C). It also shows the equilibrium temperature (417 °C), the onset temperature of the transformation on cooling, M_s (390 °C), and the onset temperature of the transformation on heating, A_s (445 °C) [6–8]. Annealings were carried out for 1 h in an argon atmosphere in order to prevent oxidation. After annealing, the specimens were air cooled (60 °C min^{-1} in the allotropic transformation temperature range).

2.3. Microscopic characterization

The microstructures were studied by optical microscopy and transmission electron microscopy. Thin foil TEM analyses were carried out using a Philips CM20 ultratwin scanning transmission electron microscope.

The thin foils were obtained by double jet electrolytic polishing with a solution of 10% perchloric acid in ethanol-2-butoxy at +5 °C (30 V). The fracture surfaces of tensile test specimens were analysed using a Jeol JSM 820 scanning electron microscope.

2.4. X-ray diffraction analysis

The X-ray diffraction patterns were obtained with a Siemens D500 diffractometer. The method applied for the quantitative determination of the proportion of α-h c p and β-f c c phases has been detailed elsewhere [4].

In brief, the method is based on the Sage and Guillaud's relationship [9]

$$\frac{x}{1-x} = k\left(\frac{I_{\beta(2\,0\,0)}}{I_{\alpha(1\,0\,\bar{1}\,1)}}\right) \quad (1)$$

TABLE I Main characteristics of both types of cobalt electrodeposit used in this study

	Type of deposits	
	1	2
Electrolysis conditions	$T = 50\,^{\circ}C$ pH > 3	$T = 50\,^{\circ}C$ pH ⩽ 3
Structure	Columnar structure	Assembly of dihedra
Texture	Very strong $\alpha(1\,1\,\bar{2}\,0)$ texture	Nearly randomly oriented
Hydrogen content	Very low	Varying; increases if pH decreases
β-fcc phase content	Nil	Varying; increases if pH decreases
Ductility	Extremely weak	Rather weak: varying; decreases if pH decreases
Surface	Satin-like or pale grey; relatively smooth	Dull dark-grey or black; Rather rough

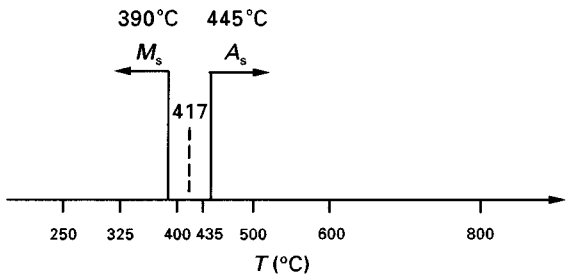

Figure 2 Summary of annealing temperatures.

in which $I_{\beta(2\,0\,0)}$ and $I_{\alpha(1\,0\,\bar{1}\,1)}$ are the measured integrated intensities of the most suitable isolated β(2 0 0) and α(1 0 $\bar{1}$ 1) diffraction peaks.

In this work, taking into account the preferred orientations frequently observed in electrodeposits, each integrated intensity was replaced in Equation 1 by the total intensity obtained from the corresponding complete pole figure. The reflection method of Schulz [10] was used to obtain experimental α(1 0 $\bar{1}$ 1) and β(2 0 0) pole figures. The complete pole figures were extrapolated from the reflection data by means of the crystallographic arguments of Scoyer *et al.* [11].

2.5. Mechanical properties

Tensile tests were performed using an Instron machine. Samples were strained at 20 °C at a crosshead speed of 0.02 cm min^{-1}. Data were measured for the 0.2% offset yield strength, $R_{e0.2\%}$, ultimate tensile strength, R_m, and per cent elongation at fracture, A. In addition, ductility measurements were made by means of a work-hardening bend test which consisted of applying cantilever bending to a strip piece clamped at one end; the specimen was bent backwards and forwards around two mandrels with a bend radius of 2 mm. This bending was repeated until fracture occurred. The bending ductility is defined as the number of cycles before fracture.

2.6. Hydrogen content determination

The hydrogen content of the cobalt electrodeposits were determined using a Leco RH1 inert gas fusion apparatus.

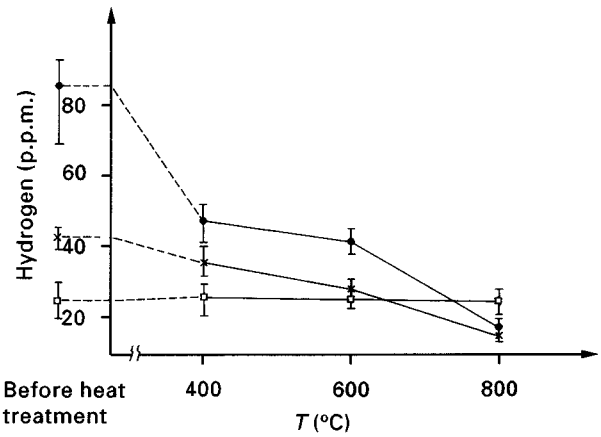

Figure 3 Hydrogen content measured after annealing for 1 h versus annealing temperature; deposits obtained at (●) pH 1, (×) pH 2, (□) pH 4.

3. Results and discussion

3.1. Hydrogen content

Fig. 3 shows the measured hydrogen contents in the deposits after annealing for 1 h at different temperatures. For the nearly randomly oriented cobalt electrodeposit obtained at pH 1.0 and pH 2.0, the hydrogen concentration decreased as the annealing temperature increased. This phenomenon can be explained most satisfactorily in terms of hydrogen detrapping during annealing. Hydrogen then escapes out of the deposit. The larger hydrogen contents found in deposits obtained at pH 1.0 should be related to the more important hydrogen co-deposition observed at this pH value.

On the other hand, the measured hydrogen content for the FT type of deposit obtained at pH 4 remained unchanged with increasing annealing temperature. In this case, the detected hydrogen probably comes from the decomposition of some occluded cobalt compound, such as $Co(OH)_2$. The occlusion of this compound during cobalt electrodeposition at high pH values has already been mentioned in the literature [12].

3.2. X-ray diffraction patterns

For the nearly randomly oriented cobalt deposits, the main change in X-ray diffraction patterns after annealing below the allotropic transformation temperature is

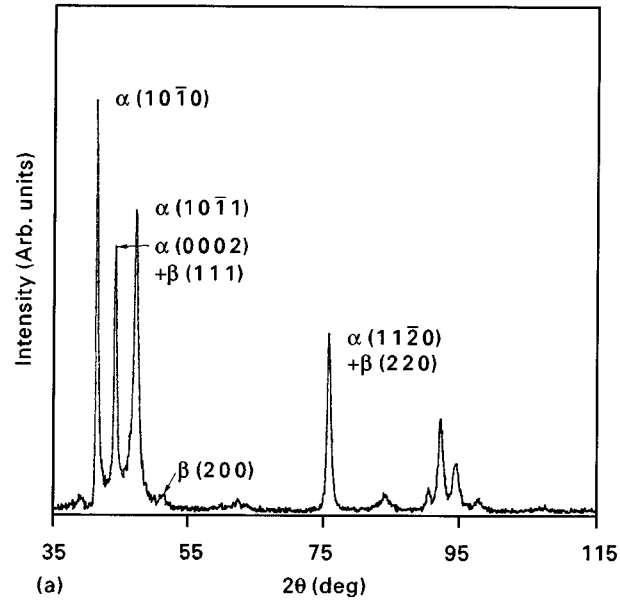

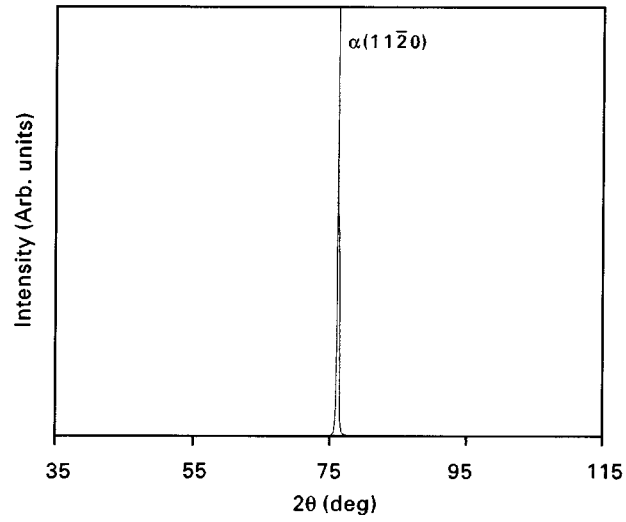

Figure 5 X-ray diffraction pattern from a deposit obtained at pH 5 and annealed 1 h at 600 °C.

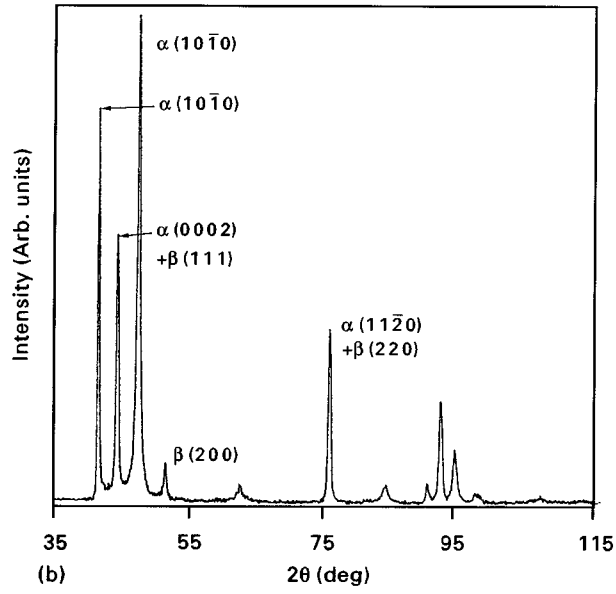

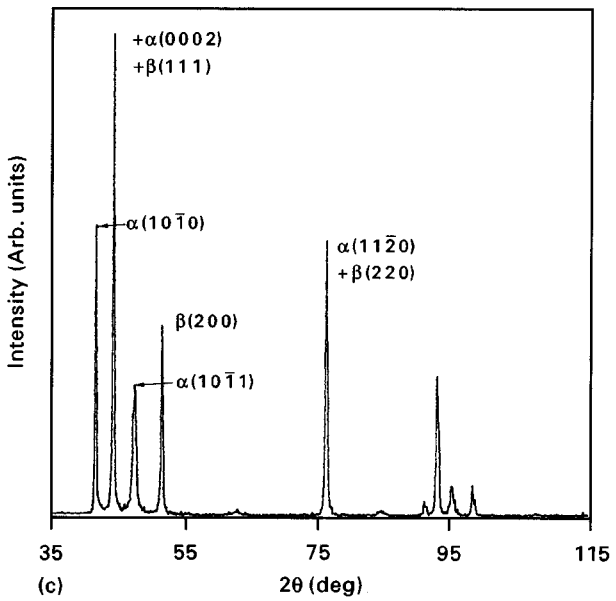

Figure 4 X ray diffraction patterns from deposits obtained at pH 1: (a) as-electrodeposited specimen; (b) specimen annealed 1 h at 400 °C; (c) specimen annealed 1 h at 600 °C.

the decrease of the α(10$\bar{1}$1) line width. As shown in Fig. 4a and b, this fact leads to an increase of the ratio: *I* maximum α(10$\bar{1}$1)/*I* maximum α(10$\bar{1}$0); the integrated intensities remaining unchanged. This phenomenon can be explained by a decrease in stacking fault density [13–15].

After annealing above the allotropic transformation temperature, the X-ray diffraction pattern of this first type of deposit reveals the retention of a significant proportion of the β-fcc phase at room temperature (see Fig. 4c).

For the X-ray diffraction patterns from field-oriented texture type of cobalt electrodeposits, only one peak, α(11$\bar{2}$0), was observed even after annealing above the allotropic transformation temperature (Fig. 5), the deposit remaining perfectly textured. This observation could be due to the reversibility of the α-hcp $\rightleftharpoons$ β-fcc transformation: an original hexagonal crystal returns identically to its former state after an α-hcp → β-fcc → α-hcp cycle. This reversibility of the α-hcp $\rightleftharpoons$ β-fcc transformation for cobalt specimens has been reported in the literature [16–18]. It should be noted that, in fact, the observed diffraction peak is a mixed [α(11$\bar{2}$0) + β(220)] peak if α and β phases coexist. Nevertheless, our pole figure investigations (Section 3.3) for the α-hcp and β-fcc volume fractions determination will show that the FT cobalt electrodeposits are always purely α-hcp. Even after annealing above the allotropic transformation temperature, the β-fcc phase volume fraction remains negligible.

3.3. Determination of the volume fractions of the α-hcp and β-fcc phases

Table II summarizes the β-fcc phase volume fraction in the deposits after annealing. For annealing temperatures below the onset temperature of the transformation on heating A_s (445 °C), no significant change in the phase volume fraction was detected.

After annealing above A_s the results were quite different depending on the type of deposit. The FT

TABLE II β-fcc phase volume fraction x in the deposits

	x (%)			
	pH 1	pH 1.5	pH 2	pH ⩾ 4
As-electrodeposited	12.5	7	5.5	< 1
Annealed at 400 °C, 1 h	12	6	4	< 1
Annealed at 435 °C, 1 h	13	7	5	< 1
Annealed at 500 °C, 1 h	59	28	17	< 1
Annealed at 600 °C, 1 h	60	27	15	< 1
Annealed at 800 °C, 1 h	29	16	4	< 1

cobalt electrodeposits remain purely α-hcp whereas the β-fcc phase content in nearly randomly oriented deposits increases markedly. After annealing in the 500 °C–600 °C temperature range, the β-fcc phase content can be as high as 60% in electrodeposits obtained at pH 1.0.

The final β-fcc content depends on the initial structure determined by the pH of the electrolysis solution and on the annealing temperature:

(i) the β-fcc content in the deposit after annealing increases as the pH of the electrolysis solution decreases;

(ii) the β-fcc content is weaker after annealing at 800 °C than after an annealing at 500 °C or 600 °C.

3.4. Microscopy investigations

After annealing below the onset temperature of the transformation on heating, A_s, no change in grain morphology and therefore no recrystallization was observed. However, TEM investigation revealed the occurrence of numerous perfect dislocations (see Fig. 6). These dislocations were not present before annealing. They result from the recombination of partial dislocations bonding a stacking fault. In hcp structure, three different kinds of stacking fault coexist and correspond to different basal plane sequences [19].

(i) intrinsic fault I_1; (0002) planes sequence ABABABACACACA
(ii) intrinsic fault I_2; (0002) planes sequence ABABABCACACA
(iii) extrinsic fault E; (0002) planes sequence ABABACBABABA

The faults I_1, I_2 and E are bounded by partial dislocations but only the partial dislocations bounding I_2 faults are glissile (Shockley type) and can recombine giving a perfect dislocation. The stacking fault then disappears. The TEM observation of these perfect dislocations confirms the previously mentioned X-ray diffraction results which indicated a decrease in stacking fault density.

Comparing Figs 7 and 8, it should be noted that even after annealing above the allotropic transformation temperature (500 or 600 °C) the grain morphology remained unchanged. This fact is due to the reversibility of the α-hcp ⇌ β-fcc transformation. On the other hand, after an annealing at 800 °C, the α-hcp → β-fcc → α-hcp cycle leads to a grain growth.

Figure 6 Transmission electron micrograph of a deposit obtained at pH 5 and annealed 1 h at 400 °C. Section parallel to the substrate.

Figure 7 Optical micrograph of an as-electrodeposited cobalt foil obtained at pH 2. Section parallel to the substrate.

For nearly randomly oriented deposits, a mixed (α-hcp + β-fcc) structure was observed. The conservation of metastable β-fcc at room temperature after annealing above the allotropic transformation temperature is a well-known phenomenon for pure cobalt. Various authors [20–22] proposed that the smaller the β-fcc crystallites before cooling, the higher is the metastable β-fcc phase content at room temperature. The results obtained in the present study and mentioned in Table II, confirm this proposition. Indeed, if the pH of the electrolysis solution decreases, it has been noted that the original α-hcp grain size – and consequently the β-fcc grain size obtained during

Figure 8 Optical micrograph of a cobalt deposit obtained at pH 2 and annealed 1 h at 600 °C. Section parallel to the substrate.

Figure 9 Transmission electron micrograph of a deposit obtained at pH 4 and annealed 1 h at 500 °C. Section parallel to the substrate.

annealing – decreases. On the other hand, an annealing at 800 °C induces grain growth.

From the results shown in Fig. 3 it also seems possible that the hydrogen remaining in the deposit during the β-fcc → α-hcp transformation on cooling stabilizes the β-fcc phase.

Figs 9 and 10 are transmission electron micrographs of thin foils parallel to the substrate for deposits annealed above the transformation temperature. Long stacking faults were observed in α-hcp phase (Fig. 9) as well as in β-fcc phase (Fig. 10).

Another important structural feature is the formation of microvoids in some deposits during annealing. These microvoids, whose size lies in the order of 500–1000 nm, were observed by optical microscopy. The microvoids were only observed in nearly randomly oriented type of deposits. From Fig. 11a–c, the following points should be noted.

(i) For deposits obtained in the same electrolysis conditions, the microvoid density after annealing increases with the annealing temperature. This is illustrated by the comparison of Fig. 11a (deposit obtained at pH 1.0 and annealed 1 h at 800 °C) and Fig. 11b (deposit obtained at pH 1.0 and annealed 1 h at 400 °C).

(ii) For a given annealing temperature, the microvoid density increases as the pH of the electrolysis solution decreases. This is illustrated by the comparison of Fig. 11a and c (deposit obtained at pH 1.5 and annealed 1 h at 800 °C).

Comparing these results with Fig. 3, it is apparent that the origin of the voids is closely connected to hydrogen: the higher the hydrogen content diffusing out of the deposit, the higher is the microvoid density.

After electrodeposition, the nearly randomly oriented deposits contain atomic hydrogen in microstructural trapping sites (dislocations, grain boundaries). A previous work [4] has shown that this trapped hydrogen does not diffuse out of the deposit at room temperature. When a specimen is heated, atomic hydrogen escapes from the traps and diffuses. As reported in the literature [23], the possibility exists that simultaneous coalescence of vacancies and the arrival of hydrogen atoms might produce microvoids containing molecular hydrogen. During its diffusion out of the deposit, molecular hydrogen temporarily agglomerates in microvoids then escapes from these traps and continues its diffusion path.

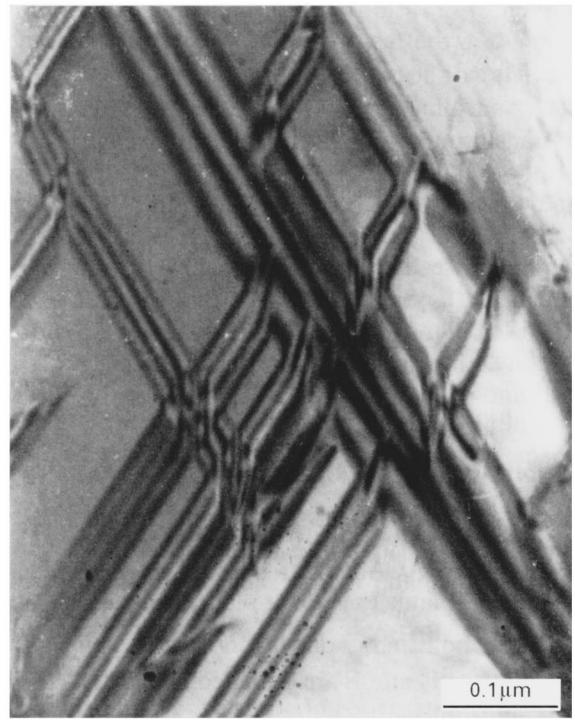

Figure 10 Transmission electron micrograph of a deposit obtained at pH 1 and annealed 1 h at 600 °C. Section parallel to the substrate.

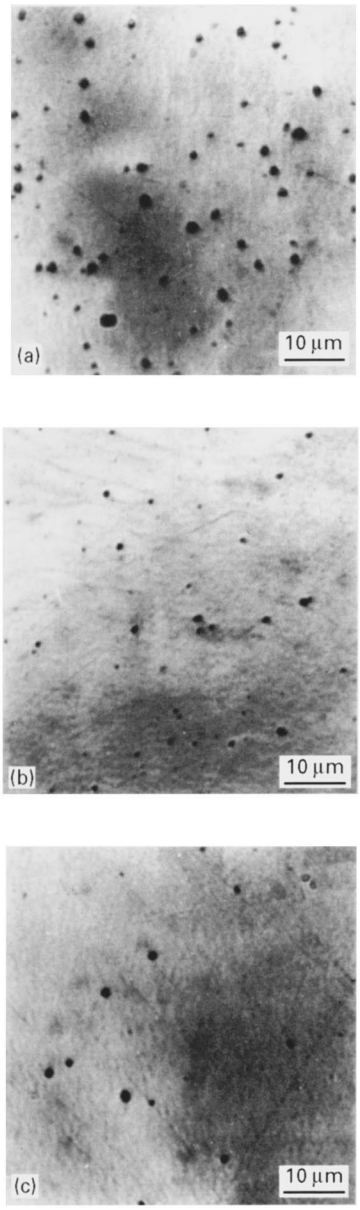

Figure 11 Optical micrographs showing microvoids. Sections parallel to the substrate: (a) deposit obtained at pH 1 and annealed 1 h at 800 °C; (b) deposit obtained at pH 1 and annealed 1 h at 400 °C; (c) deposit obtained at pH 1.5 and annealed 1 h at 800 °C.

After annealing, the deposit contains micro-voids which are an indelible mark of hydrogen out-diffusion.

3.5. Mechanical properties

Fig. 12a–c shows tensile curves illustrating the effect of annealing treatments on the mechanical behaviour characteristics of different types of deposit.

For deposits obtained at pH 1 (Fig. 12a), the increase in ductility after annealing is negligible. The high β-f c c content in these deposits after an annealing above the allotropic transformation does not correspond to an improvement of ductility, as was expected. This fact can be explained by the indirect role of hydrogen affecting the ductility by forming microvoids which may act as sites for fracture nucleation. During tension tests, microvoid coalescence induces a premature fracture and so annealing does not improve the ductility of this kind of deposit. This role of hydrogen was mentioned previously by Zeller and Landau in electrodeposited Ni–P amorphous alloys [24].

It should be noted that SEM observations of the fracture surface of deposits obtained at pH 1 reveal completely different aspects from the electrodeposited specimen and the annealed specimen. The fracture surface of an as-electrodeposited specimen exhibits a quasi-cleavage fracture aspect (Fig. 13); on the other hand, for the annealed specimen, microvoid coalescence leaves behind on the fracture surface the familiar hemispheroidal cavities that are known as dimples (Fig. 14).

An increase in ductility after annealing is observed for the nearly randomly oriented deposit obtained at pH 1.5 (Fig. 12b) or, to a lower extent, obtained at pH 2. The reason for the beneficial effect of annealing is not fully understood. As the microvoid density after annealing decreases when the hydrogen content of the electrodeposited foil decreases, the detrimental effect of hydrogen out-diffusion during annealing is limited for deposits obtained at pH higher than 1.0.

On the other hand, two structural changes observed after annealing could open the way to ductility improvement:

(i) decrease of the stacking fault density,

(ii) after annealing above the allotropic transformation temperature, the increase of β-f c c phase content.

For strongly textured cobalt electrodeposits (obtained at pH > 3.0), annealing induces a dramatic improvement of the ductility (Fig. 12c). This field oriented texture type of deposit exhibits a total lack of ductility in as-electrodeposited conditions ($A < 1\%$). After annealing, its elongation at fracture increases up to about 8% (annealing 1 h at 400 °C) or, even, up to 12% (annealing 1 h at 600 °C). It appears clearly from this study that the ductility improvement cannot be due to the following factors: hydrogen evolution, β-f c c content increase, grain morphology modification or texture modification. For the strongly textured type of deposit, the only structural change observed after annealing and leading to an increase of the ductility is the decrease of the stacking fault density.

The tensile ductilities characterized by the per cent elongation at fracture, A, are listed in Table III for various electrolysis conditions and annealing temperatures. These results are confirmed by the work-hardening bend tests (see Table IV). To sum up, an important improvement of the cobalt foil ductility is observed after annealing, except for deposits obtained at pH 1.0.

4. Conclusion

The effects of annealing treatments on the structure and mechanical properties of thick cobalt electrodeposits were studied. It can be concluded that annealing is a very effective means to optimize the ductility of cobalt electrodeposits. The increase in ductility observed after annealing is essentially due to a decrease of the stacking fault density in the deposit.

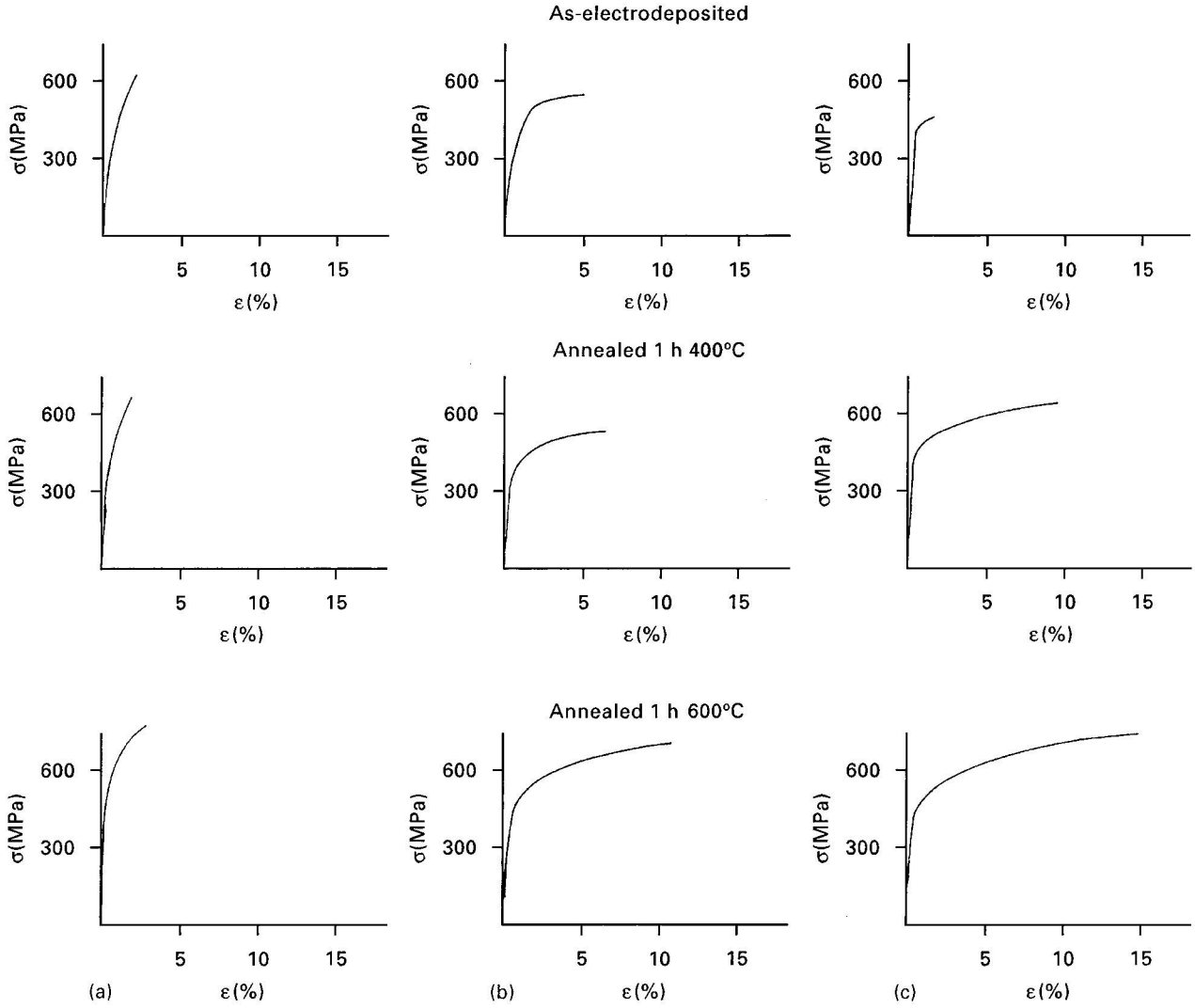

Figure 12 Engineering stress–strain curves: deposits obtained at (a) pH 1, (b) pH 1.5, (c) pH 4.

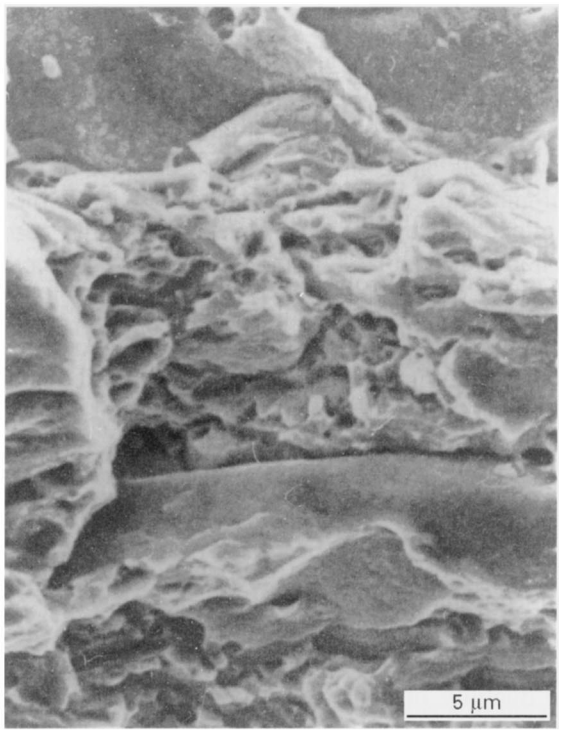

Figure 13 SEM image of the fracture surface for an as-electrodeposited specimen obtained at pH 1.

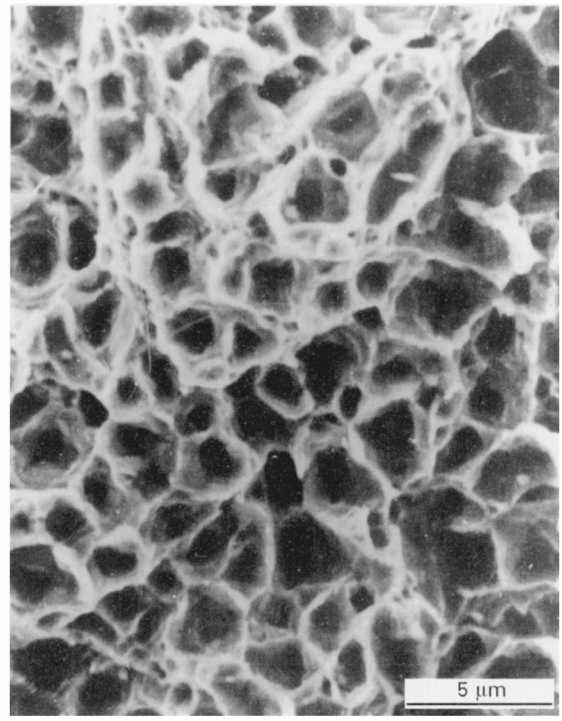

Figure 14 SEM image of the fracture surface for a deposit obtained at pH 1 and annealed 1 h at 800 °C.

Table III Tensile test results: per cent elongation at fracture, A

	A (%)				
	pH 1	pH 1.5	pH 2	pH 4	pH 5
As-electrodeposited	2.1	2.8	5.1	0.8	0.3
Annealed at 250 °C, 1 h	2	3.5	7	8.4	6.1
Annealed at 400 °C, 1 h	2.1	5.8	7	8.5	9
Annealed at 500 °C, 1 h	1.7	10.7	7.9	12.3	12.2
Annealed at 600 °C, 1 h	2.5	10.8	7.8	14.3	13
Annealed at 800 °C, 1 h	2	12.2	7.3	12.2	13.7

TABLE IV Work-hardening bend-test results: number of bends before fracture (bend radius = 2 mm)

	No. of bends			
	pH 1	pH 1.5	pH 2	pH 4
As-electrodeposited	2	6	15	0
Annealed at 400 °C, 1 h	5	39	48	54
Annealed at 600 °C, 1 h	5	57	42	63
Annealed at 800 °C, 1 h	3	53	53	61

Annealing treatment above the allotropic transformation temperature (417 °C) also produces an increase of the ductile β-f c c phase content in cobalt electrodeposits obtained at 50 °C and pH < 3.0. These higher β-f c c phase contents do not lead (contrary to what was expected) to supplementary improvements of ductility. This fact can be explained by the role of incorporated hydrogen always existing in such deposits. During annealing, the out-diffusion of hydrogen induces the formation of microvoids which act as sites for fracture nucleation. For this reason, the maximum ductility after annealing treatment of pure cobalt electrodeposits corresponds to the intrinsic ductility of cobalt α-h c p phase and is comparable to the ductility of pure cobalt foils obtained by thermomechanical processes.

In order to gain from the higher ductility of the β-f c c phase, it is necessary first to produce an as-electrodeposited foil free of incorporated hydrogen and, then, to obtain a significant β-f c c phase content after annealing. The present work has shown that this seemed to be very difficult for pure cobalt. However, it would be interesting to investigate in a further study if the co-deposition of iron or nickel (which stabilize the β-f c c phase) permits that objective to be reached.

References

1. F. DIDERICH, J. M. DRAPIER, D. COUTSOURADIS and L. HABRAKEN, *Le Cobalt* **1** (1975) 7.
2. R.W. FRASER, D. J. L. EVANS and V.N. MACKIW, *Cobalt* **25** (1964) 72.
3. M. BECKERS, L. FONTAINAS, B. TOUGARINOFF and L. HABRAKEN, *ibid.* **25** (1964) 171.
4. J. DILLE, J. CHARLIER and R. WINAND, *J. Mater. Sci.* **32** (1997) 2637.
5. J. DILLE, PhD thesis, Université Libre de Bruxelles (1994).
6. W. KRAJEWSKI, J. KRUGER and H. WINTERHAGER, *Metall* **27** (1973) 480.
7. J. C. ZHAO and M. R. NORIS, *Scripta Metall. Mater.* **32** (1995) 1671.
8. H. BIBRING and F. SEBILLEAU, *Rev. Metall.* **52** (1955) 569.
9. M. SAGE and Ch. GUILLAUD, *ibid.* **47** (1950) 139.
10. L. G. SCHULTZ, J. *Appl. Phys.* **20** (1949) 1030.
11. J. SCOYER, R. WINAND and J. CHARLIER, *ATB Métall.* **15** (1975) 222.
12. S. NAKARHARA and S. MAHAJAN, *J. Electrochem. Soc.* **127** (1980) 283.
13. B. E. WARREN, "X-ray diffraction" (Addison-Wesley, Reading, MA, 1969).
14. C. R. HOUSKA and B. L. AVERBACH, *Acta Crystallogr.* **2** (1958) 139.
15. C. R. HOUSKA, B. L. AVERBACH and M. COHEN, *Acta Metall.* **8** (1960) 81.
16. H. BIBRING, F. SEBILLEAU and C. BÜCKLE, *J. Inst. Metals* **87** (1959) 71.
17. J. O. NELSON and C. J. ALTSLETTER, *Trans. Met. Soc. AIME* **230** (1964) 1577.
18. R. ADAMS and C. J. ALTSLETTER, *ibid.* **242** (1968) 139.
19. J. P. HIRTH and J. LUTHE, "Theory of dislocations" (McGraw-Hill, New York, 1968).
20. A. R. TROIANO and J. L. TOKICH, *Trans. Met. Soc. AIME* **175** (1948) 728.
21. O. S. EDWARDS and H. LIPSON, *J. Inst. Metals* **69** (1943) 177.
22. G. BOUQUET and B. DUBOIS, *Scripta Metall.* **12** (1978) 1079.
23. S. NAKAHARA, *Acta Metall.* **36** (1988) 1669.
24. R. L. ZELLER and U. LANDAU, *J. Electrochem. Soc.* **137** (1990) 1107.

Received 15 September 1997
and accepted 3 March 1998